Statistical Analysis of Random Telegraph Noise in CMOS Image Sensors

Jun-Myung Woo, Hong-Hyun Park, Hong Shick Min and Young June Park
School of EECS and Nano-Systems Institute (NSI-NCRC)
Seoul National University
Seoul, Korea
E-mail: woojm99@isis.snu.ac.kr

Sung-Min Hong and Chan Hyeong Park*
EIT4
Bundeswehr University
Neubiberg, Germany
*Department of ECE
Kwangwoon University
Seoul, Korea

***Abstract*—We propose a statistical method to predict the dark random readout noise in CMOS image sensors. First, we calculate the dark random noise originated from oxide traps present in the source-follower MOSFET. Statistical variation in the dark noise is associated with the random variation of the oxide defects in the CMOS image sensor cells in both the energy and space domain. Considering the effect of the correlated double sampling, we define the dark random noise as the standard deviation in the time domain and analyze the effect of the MOSFET width and length variations and temperature on its dark random noise.**

Keywords - CMOS image sensor (CIS), random telegraph noise (RTN), oxide trap, correlated double sampling (CDS), dark random noise

I. INTRODUCTION

One of the most serious noise sources in a CMOS image sensor (CIS) pixel is due to oxide traps in a source-follower MOSFET. Carrier trapping process into oxide traps is usually thought to be the physical origin of $1/f$ noise in MOSFETs and becomes random telegraph signal (RTS) noise as the device scales down to submicron scale. Recent research [1] found out that statistical variations in oxide defects are the cause of the pixels having very large noise, which is represented as a long tail in a dark readout noise histogram. Thus, it is important to have statistical simulation capability to predict the noise characteristics from the gate oxide quality. For a statistical noise analysis, we consider a conventional 4-transistor CIS pixel as shown in Fig. 1.

As a statistical sample, we take 10,000 source-follower MOSFETs, each having traps according to the Poisson distribution in the total number of traps. To consider the CDS effect, noise analysis in the time domain has been performed. From the RTS characteristics, the dark random noise after CDS for each cell transistor is calculated and the noise histogram is plotted.

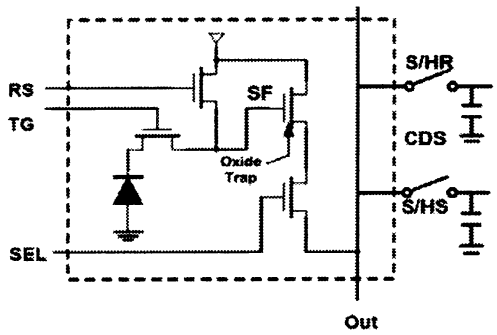

Figure 1. Circuit schematic of 4-transistor CIS pixel. Oxide traps are distributed in the source follower MOSFET for the dark random noise simulation.

II. RANDOM TELEGRAPH SIGNAL CHARACTERISTICS

As shown in Fig. 2, the RTS noise can be characterized by τ_c, τ_e and ΔI, i.e. average times for capture and emission of electrons and associated drain current change, respectively. Once the energy and the spatial position of a trap are defined, we can derive the RTS characteristics as follows. Let T be the probability for tunneling, z be the distance from Si-SiO_2 interface and τ_0 be the tunneling time constant of the electron. From τ_0, we can get the capture time τ_c and the emission time τ_e as follows:

$$T = \exp(-\alpha z) \propto \frac{1}{\tau_0} \tag{1}$$

$$\tau_c = \frac{1}{2}\frac{\tau_0}{f(E_T)}, \quad \tau_e = \frac{1}{2}\frac{\tau_0}{1-f(E_T)} \tag{2}$$

$$\text{where } f(E_T) = \frac{1}{1+\exp[(E_T - E_F)/k_B T]}. \tag{3}$$

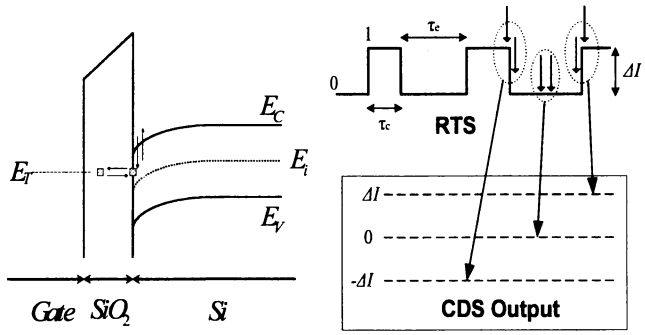

Figure 2. Energy band diagram that illustrates RTS noise caused by a possible carrier transition. Three cases of RTS transitions during CDS and corresponding CDS outputs.

This is consistent with the well-known equation for capture time as $\tau_e = (\tau_c / g)\exp[-(E_T - E_F)/k_BT]$ [2]. Finally, ΔI can be calculated by the Green's function approach reported in [3][4]. For the calculation of ΔI, the mobility fluctuations due to the trapped charge are neglected in this work.

III. The Effect of Correlated Double Sampling

During the pixel readout period, the pixel samples a reference value first. After the charge transfer, the pixel samples the video signal. By subtracting these two samples, the correlated offset is cancelled so that only the photo-integrated charges appear as the CDS output. If no charge transfers, that is, in dark condition, the CDS output should be 0. However, when the transition of the current due to the RTS occurs between two samplings, the CDS output is disturbed.

A. Case of a Single Trap

We define the dark random noise as a standard deviation of the CDS output. Let P_0 and P_1 be the probability of finding state 0 and state 1, respectively, in arbitrary time and $P_{ab}(t)$ be the probability of the transition from state a to state b during time t.

$$P_0 = \frac{\tau_e}{\tau_e + \tau_c}, \quad P_1 = \frac{\tau_c}{\tau_e + \tau_c} \tag{4}$$

$$P_{00}(t) = P_0 + P_1 \times \exp\left[-t\left(\frac{1}{\tau_e} + \frac{1}{\tau_c}\right)\right] \tag{5}$$

$$P_{11}(t) = P_1 + P_0 \times \exp\left[-t\left(\frac{1}{\tau_e} + \frac{1}{\tau_c}\right)\right] \tag{6}$$

P_{01} and P_{10} can be derived from the total probability relations.

$$P_{00} + P_{01} = P_{10} + P_{11} = 1 \tag{7}$$

In the case of a single trap, CDS output has three discrete values, i.e. ΔI, 0 and $-\Delta I$. From the probability of each state and the transition probability, the probability of each CDS output value can be derived. Letting T_S be the sampling time interval,

$$P(x = \Delta I) = P_0 \times P_{01}(T_S) \tag{8a}$$

$$P(x = 0) = P_0 \times P_{00}(T_S) + P_1 \times P_{11}(T_S) \tag{8b}$$

$$P(x = -\Delta I) = P_1 \times P_{10}(T_S) \tag{8c}$$

For the noise analysis, we calculate the standard deviation of the CDS output.

$$\sigma_x = \sqrt{\sum_i x_i^2 P(x_i) - \langle x \rangle^2}$$
$$\text{where } \langle x \rangle = \sum_i x_i P(x_i) \tag{9}$$

B. Case of Multiple Traps

We can extend the above formulation to a multiple-trap situation. Considering N traps in the oxide, the transition probability from the (α_1, α_2, α_3, ... ,α_N; t=0) state to the (β_1, β_2, β_3, ... ,β_N; t=T_S) state is

$$P_k = \prod_{k=1}^{N} P_{\alpha n} \times P_{\alpha\beta n}. \tag{10}$$

The α and β can be 0 or 1. Letting Y be the CDS output, the corresponding CDS output is

$$Y_k = \sum_{n=1}^{N} D_{\alpha\beta n} \times \Delta I_n,$$

$$\text{where } D_{\alpha\beta n} = \begin{cases} 1 & if\ \beta_n > \alpha_n \\ 0 & if\ \beta_n = \alpha_n \\ -1 & if\ \beta_n < \alpha_n \end{cases}. \tag{11}$$

In the case of N traps, the number of the observable CDS outputs is 3^N. We calculate the standard deviation of the CDS output from 3^N CDS outputs and corresponding probability.

$$\sigma_Y = \sqrt{\sum_{k=1}^{3^N} Y_k^2 P_k - \left(\sum_{k=1}^{3^N} Y_k P_k\right)^2}. \tag{12}$$

IV. Simulation Results and Discussion

As the source-follower transistor, a conventional planar MOSFET is considered in the simulation. The gate channel length is set to 0.32 μm and the oxide thickness is 65 Å. The bias condition of the source follower is set by dark read-out condition. We generated 10,000 samples of source follower MOSFETs. In the oxide of each sample, traps are randomly distributed, that is, the number of traps in each MOSFET follows the Poisson distribution. In this simulation, the oxide trap density per unit energy is set to be 2×10^{16} cm^{-3} eV^{-1}, uniform in both energy and space.

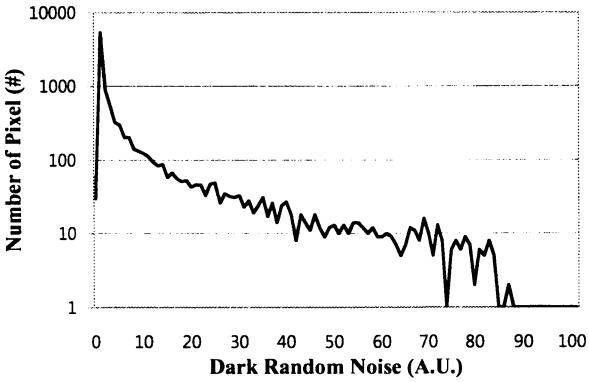

Figure 3. Dark random noise histogram of 10,000 pixels. The width is 0.2 μm.

We calculate deviations from τ_c, τ_e and ΔI in each trap of MOSFET. Fig. 3 shows the dark random noise histogram of the pixels. As can be seen in Fig. 3, the noise histogram has a long tail, which has a similar shape to the experimental data [1]. The difference in the peak value between simulation and experimental results may be due to the effects from thermal noise, which is neglected in this work [1].

With the same oxide trap density, as the gate area increases, the source-follower MOSFET has more traps and larger dark random noise. Fig. 4 shows the noise histogram of 0.4 μm, 0.2 μm and 0.1 μm in width. As the channel width becomes narrower, the tail gets thinner and shorter, which means that there are less noisy pixels. In Fig. 5, we reproduce dark random noise on 100×100 pixels. We can see more white pixels in dark condition as the channel width increases.

As devices scales down, it is important to predict the tendency of its influence on the random dark noise. We simulate the source-follower MOSFETs whose channel length is 0.32 μm, 0.18 μm and 0.13 μm, and oxide thickness is 100 Å, 50 Å and 34 Å, respectively. The channel width is set to be 0.2 μm in common.

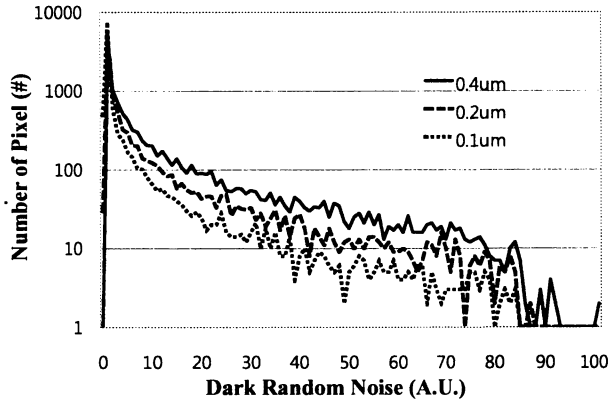

Figure 4. Dark random noise histogram of 10,000 pixels with the channel-width variation. As the width decreases, tail gets thinner and shorter.

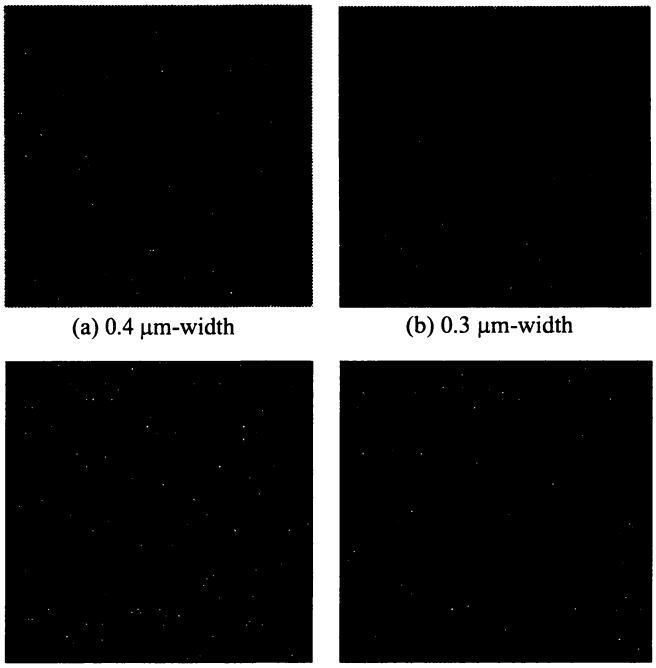

(a) 0.4 μm-width (b) 0.3 μm-width

(c) 0.2 μm-width (d) 0.1 μm-width

Figure 5. Reproduced 100×100 pixels. White dots mean noisy pixels.

We generated 10,000 samples of source-follower MOSFETs in each case. The oxide trap density per unit energy is set to be 2×10^{16} cm^{-3} eV^{-1}, uniform in both energy and space.

Fig. 6 shows noise histogram with the channel length variation. As the channel length becomes shorter, the noise histogram has a much longer tail, which means that there are more large noisy pixels.

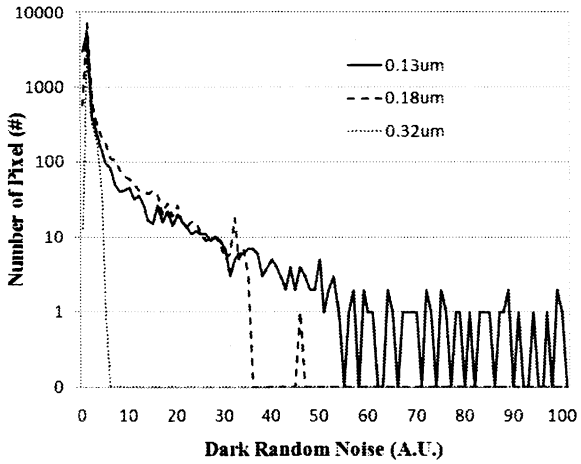

Figure 6. Dark random noise histogram of 10,000 pixels with the channel-length variation. As the length decreases, a tail becomes much longer. The channel width is set to be 0.2 μm in common.

The short channel device has less oxide traps with the same oxide trap density. However, once the electron is trapped in the oxide trap, it is more effective in changing the drain current, i.e. RTS amplitude ΔI than in the long-channel device. In Fig. 7, we can compare the Green's function in the oxide of two devices whose channel length is 0.32 μm and 0.13 μm. The short channel device has a much larger value of Green's function. Therefore, RTS amplitude ΔI is much larger in the short-channel device. This is why the noise histogram of the short-channel device has a longer tail than that of the long-channel device noise histogram.

Fig. 8 shows the dark random noise dependency on temperature. We note that the average value of the dark random noise increases with temperature.

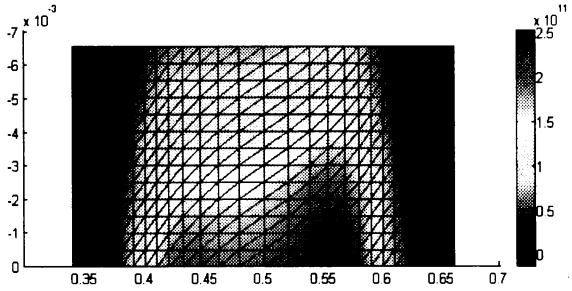

(a) 0.32 μm-length

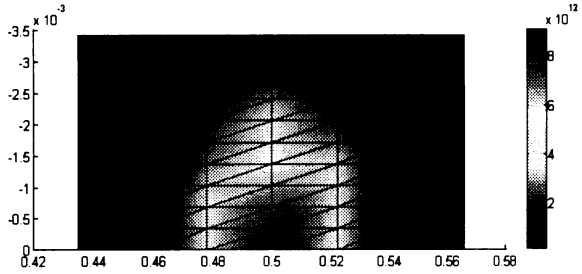

(b) 0.13 μm-length

Figure 7. Calculated Green's function in the oxide of each device. This value means the drain current change per unit charge injection into the device. The short-channel device has a larger value of Green's function compared with that of the long-channel device.

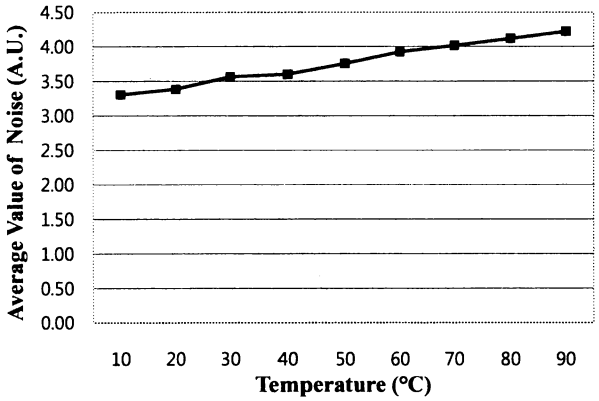

Figure 8. Calculated average noise dependency on temperature.

V. Conclusion

In this work, we have statistically analyzed the dark random noise of CIS output. From the RTS characteristics of each oxide trap, the standard deviation is calculated in the time domain in order to include the CDS effect. Ten-thousand samples of pixels have been simulated and the effects of the width and length variations on the statistical nature of the RTS noise have been analyzed.

Acknowledgment

This work was supported by the NCRC program of the KOSEF through the NSI at Seoul National University and Samsung Electronics Company. C. H. Park's work has been supported by Nano IP/SoC Promotion Group of Seoul R&BD Program in 2008.

References

[1] X. Wang, P. R. Rao, A. Mierop and A. J. P. Theuwissen, "Random Telegraph Signal in CMOS Image Sensor Pixels," in *IEDM Tech. Dig.*, 115 (2006).

[2] M. J. Kirton, M. J. Uren, S. Collins, M. Schulz, A. Karmann, and K. Scheffer, "Individual Defects at the Si:SiO_2 Interface," *Semicon. Sci. Technol.* **4**, 1116 (1989).

[3] F. Bonani, S. D. Guerrieri, G. Ghione and M. Pirola, "A TCAD Approach to the Physics-Based Modeling of Frequency Conversion and Noise in Semiconductor Devices under Large-Signal Forced Operation," *IEEE Trans. Electron Devices* **48**, 966 (2001).

[4] S. -M. Hong, H. -H. Park, C. H. Park, M. J. Lee, H. S. Min and Y. J. Park, "Physics-Based Simulation of 1/*f* Noise in MOSFETs under Large-Signal Operation," in *12th International Conference on Simulation of Semiconductor Processes and Devices*, 89 (2007).